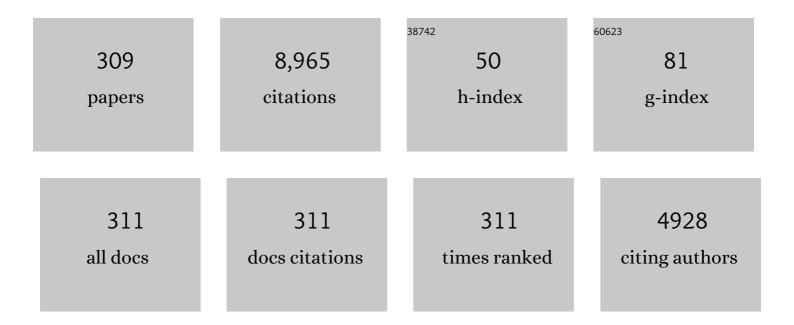
List of Publications by Year in descending order

Source: https://exaly.com/author-pdf/594727/publications.pdf Version: 2024-02-01



#	Article	IF	CITATIONS
1	Size–strain line-broadening analysis of the ceria round-robin sample. Journal of Applied Crystallography, 2004, 37, 911-924.	4.5	417
2	ENGIN-X: a third-generation neutron strain scanner. Journal of Applied Crystallography, 2006, 39, 812-825.	4.5	293
3	Use of Rietveld refinement for elastic macrostrain determination and for evaluation of plastic strain history from diffraction spectra. Journal of Applied Physics, 1997, 82, 1554-1562.	2.5	291
4	Lattice strain evolution during uniaxial tensile loading of stainless steel. Materials Science & Engineering A: Structural Materials: Properties, Microstructure and Processing, 1999, 259, 17-24.	5.6	258
5	Hydrogen in zirconium alloys: A review. Journal of Nuclear Materials, 2019, 518, 440-460.	2.7	203
6	Measuring strain distributions in amorphous materials. Nature Materials, 2004, 4, 33-36.	27.5	199
7	Elastoplastic deformation of ferritic steel and cementite studied by neutron diffraction and self-consistent modelling. Acta Materialia, 2002, 50, 1613-1626.	7.9	173
8	The determination of a continuum mechanics equivalent elastic strain from the analysis of multiple diffraction peaks. Journal of Applied Physics, 2004, 96, 4263-4272.	2.5	151
9	Interphase and intergranular stress generation in carbon steels. Acta Materialia, 2004, 52, 1937-1951.	7.9	149
10	Incorporation of twinning into a crystal plasticity finite element model: Evolution of lattice strains and texture in Zircaloy-2. International Journal of Plasticity, 2011, 27, 1721-1738.	8.8	136
11	On the measurement of dislocations and dislocation substructures using EBSD and HRSD techniques. Acta Materialia, 2019, 175, 297-313.	7.9	128
12	Load partitioning between ferrite and cementite during elasto-plastic deformation of an ultrahigh-carbon steel. Acta Materialia, 2007, 55, 1999-2011.	7.9	123
13	In situ study of hydride precipitation kinetics and re-orientation in Zircaloy using synchrotron radiation. Acta Materialia, 2010, 58, 6575-6583.	7.9	122
14	Strain imaging by Bragg edge neutron transmission. Nuclear Instruments and Methods in Physics Research, Section A: Accelerators, Spectrometers, Detectors and Associated Equipment, 2002, 481, 765-768.	1.6	119
15	Measured and predicted intergranular strains in textured austenitic steel. Acta Materialia, 2000, 48, 553-564.	7.9	111
16	On the diffractive determination of single-crystal elastic constants using polycrystalline samples. Journal of Applied Crystallography, 2001, 34, 585-601.	4.5	105
17	Strain and texture evolution during mechanical loading of a crack tip in martensitic shape-memory NiTi. Acta Materialia, 2007, 55, 3929-3942.	7.9	105
18	Texture inheritance and variant selection through an hcp–bcc–hcp phase transformation. Acta Materialia, 2010, 58, 4053-4066.	7.9	105

#	Article	IF	CITATIONS
19	On the deformation twinning of Mg AZ31B: A three-dimensional synchrotron X-ray diffraction experiment and crystal plasticity finite element model. International Journal of Plasticity, 2015, 70, 77-97.	8.8	103
20	Use of Rietveld refinement to fit a hexagonal crystal structure in the presence of elastic and plastic anisotropy. Journal of Applied Physics, 1999, 85, 739-747.	2.5	102
21	Modeling lattice strain evolution during uniaxial deformation of textured Zircaloy-2. Acta Materialia, 2008, 56, 3672-3687.	7.9	97
22	In situ neutron diffraction studies of martensitic transformations in NiTi polycrystals under tension and compression stress. Materials Science & Engineering A: Structural Materials: Properties, Microstructure and Processing, 2004, 378, 97-104.	5.6	86
23	Evidence of variation in slip mode in a polycrystalline nickel-base superalloy with change in temperature from neutron diffraction strain measurements. Acta Materialia, 2007, 55, 3089-3102.	7.9	85
24	Deformation behaviour of an advanced nickel-based superalloy studied by neutron diffraction and electron microscopy. Acta Materialia, 2012, 60, 6829-6841.	7.9	82
25	Evaluating zirconium–zirconium hydride interfacial strains by nano-beam electron diffraction. Journal of Nuclear Materials, 2013, 432, 366-370.	2.7	80
26	Multi-scale modeling and experimental study of twin inception and propagation in hexagonal close-packed materials using a crystal plasticity finite element approach—Part I: Average behavior. Journal of the Mechanics and Physics of Solids, 2013, 61, 783-802.	4.8	78
27	Internal strain and texture development during twinning: Comparing neutron diffraction measurements with crystal plasticity finite-element approaches. Acta Materialia, 2012, 60, 2240-2248.	7.9	75
28	High-temperature deformation mechanisms in a polycrystalline nickel-base superalloy studied by neutron diffraction and electron microscopy. Acta Materialia, 2014, 74, 18-29.	7.9	75
29	Multi-scale modeling and experimental study of twin inception and propagation in hexagonal close-packed materials using a crystal plasticity finite element approach; part II: Local behavior. Journal of the Mechanics and Physics of Solids, 2013, 61, 803-818.	4.8	71
30	A finite element model of deformation twinning in zirconium. Materials Science & Engineering A: Structural Materials: Properties, Microstructure and Processing, 2008, 473, 139-146.	5.6	70
31	Neutron-diffraction study of stress-induced martensitic transformation in TRIP steel. Applied Physics A: Materials Science and Processing, 2002, 74, s1143-s1145.	2.3	68
32	Texture and strain analysis of the ferroelastic behavior of Pb(Zr,Ti)O3 byin situneutron diffraction. Journal of Applied Physics, 2003, 93, 4104-4111.	2.5	68
33	In situ study of defect accumulation in zirconium under heavy ion irradiation. Journal of Nuclear Materials, 2013, 433, 95-107.	2.7	65
34	Development of internal strains in textured Zircaloy-2 during uni-axial deformation. Materials Science & Engineering A: Structural Materials: Properties, Microstructure and Processing, 2008, 488, 172-185.	5.6	64
35	Effect of thermo-mechanical cycling on zirconium hydride reorientation studied in situ with synchrotron X-ray diffraction. Journal of Nuclear Materials, 2013, 440, 586-595.	2.7	64
36	Evolution of dislocation structure in neutron irradiated Zircaloy-2 studied by synchrotron x-ray diffraction peak profile analysis. Acta Materialia, 2017, 126, 102-113.	7.9	63

#	Article	IF	CITATIONS
37	A virtual laboratory for neutron and synchrotron strain scanning. Physica B: Condensed Matter, 2004, 350, E743-E746.	2.7	61
38	Modeling the room temperature deformation of a two-phase zirconium alloy. Acta Materialia, 2009, 57, 407-419.	7.9	61
39	Study of 3-D stress development in parent and twin pairs of a hexagonal close-packed polycrystal: Part Il – crystal plasticity finite element modeling. Acta Materialia, 2015, 93, 235-245.	7.9	61
40	Study on the effects of matrix yield strength on hydride phase stability in Zircaloy-2 and Zr 2.5wt% Nb. Journal of Nuclear Materials, 2012, 425, 93-104.	2.7	59
41	Microstrain evolution during creep of a high volume fraction superalloy. Materials Science & Engineering A: Structural Materials: Properties, Microstructure and Processing, 2005, 399, 141-153.	5.6	57
42	Dislocation structure evolution induced by irradiation and plastic deformation in the Zr–2.5Nb nuclear structural material determined by neutron diffraction line profile analysis. Acta Materialia, 2012, 60, 5567-5577.	7.9	56
43	Study of 3-D stress development in parent and twin pairs of a hexagonal close-packed polycrystal: Part I – in-situ three-dimensional synchrotron X-ray diffraction measurement. Acta Materialia, 2015, 93, 246-255.	7.9	56
44	An optimum design for a time-of-flight neutron diffractometer for measuring engineering stresses. Journal of Applied Crystallography, 2002, 35, 49-57.	4.5	55
45	Elastoplastic deformation of 316 stainless steel under tensile loading at elevated temperatures. Metallurgical and Materials Transactions A: Physical Metallurgy and Materials Science, 2006, 37, 1863-1873.	2.2	55
46	Lattice strain evolution during cyclic loading of stainless steel. Acta Materialia, 2002, 50, 1627-1638.	7.9	54
47	Intergranular strain accumulation in a near-alpha titanium alloy during plastic deformation. Acta Materialia, 2002, 50, 4847-4864.	7.9	54
48	Strain evolution of zirconium hydride embedded in a Zircaloy-2 matrix. Journal of Nuclear Materials, 2008, 380, 70-75.	2.7	53
49	A synchrotron radiation study of transient internal strain changes during the early stages of thermal cycling in an Al / SiCw MMC. Scripta Materialia, 1996, 35, 1229-1234.	5.2	52
50	Comparison of residual strains measured by X-ray and neutron diffraction in a titanium (Ti–6Al–4V) matrix composite. Materials Science & Engineering A: Structural Materials: Properties, Microstructure and Processing, 1999, 259, 209-219.	5.6	52
51	Modeling discrete twin lamellae in a microstructural framework. Scripta Materialia, 2016, 121, 84-88.	5.2	52
52	NON-DESTRUCTIVE INVESTIGATION OF BRONZE ARTEFACTS FROM THE MARCHES NATIONAL MUSEUM OF ARCHAEOLOGY USING NEUTRON DIFFRACTION*. Archaeometry, 2006, 48, 77-96.	1.3	51
53	Fast residual stress mapping using energy-dispersive synchrotron X-ray diffraction on station 16.3 at the SRS. Journal of Synchrotron Radiation, 2002, 9, 77-81.	2.4	49
54	Measurement of strain in a titanium linear friction weld by neutron diffraction. Physica B: Condensed Matter, 2003, 325, 130-137.	2.7	49

#	Article	IF	CITATIONS
55	Modeling texture evolution during uni-axial deformation of Zircaloy-2. Journal of Nuclear Materials, 2009, 394, 9-19.	2.7	49
56	Effect of neutron irradiation on deformation mechanisms operating during tensile testing of Zr–2.5Nb. Acta Materialia, 2016, 102, 352-363.	7.9	48
57	A solution to FIB induced artefact hydrides in Zr alloys. Journal of Nuclear Materials, 2019, 515, 122-134.	2.7	48
58	â€~Time-resolved and orientation-dependent electric-field-induced strains in lead zirconate titanate ceramics. Applied Physics Letters, 2007, 90, 172909.	3.3	47
59	Indentation size effect, geometrically necessary dislocations and pile-up effects in hardness testing of irradiated nickel. Acta Materialia, 2021, 207, 116702.	7.9	47
60	Evaluation of elastic–viscoplastic self-consistent polycrystal plasticity models for zirconium alloys. International Journal of Solids and Structures, 2015, 71, 308-322.	2.7	46
61	Evidence for basal ã€^a〉-slip in Zircaloy-2 at room temperature from polycrystalline modeling. Journal of Nuclear Materials, 2008, 373, 217-225.	2.7	44
62	The precision of diffraction peak location. Journal of Applied Crystallography, 2001, 34, 737-743.	4.5	43
63	Intergranular stresses in polycrystalline fatigue: diffraction measurement and self-consistent modelling. Engineering Fracture Mechanics, 2004, 71, 805-812.	4.3	43
64	Elastic phase-strain distribution in a particulate-reinforced metal-matrix composite deforming by slip or creep. Metallurgical and Materials Transactions A: Physical Metallurgy and Materials Science, 1999, 30, 2989-2997.	2.2	42
65	A comparison between Engin and Engin-X, a new diffractometer optimized for stress measurement. Physica B: Condensed Matter, 2004, 350, E511-E514.	2.7	42
66	Evolution of interphase and intergranular stresses in Zr–2.5Nb during room temperature deformation. Materials Science & Engineering A: Structural Materials: Properties, Microstructure and Processing, 2009, 501, 166-181.	5.6	39
67	Deformation of high β-phase fraction Zr–Nb alloys at room temperature. Acta Materialia, 2012, 60, 3355-3369.	7.9	39
68	Microstructure characterization of a hydride blister in Zircaloy-4 by EBSD and TEM. Acta Materialia, 2017, 129, 450-461.	7.9	39
69	Molecular dynamics simulations of irradiation cascades in alpha-zirconium under macroscopic strain. Nuclear Instruments & Methods in Physics Research B, 2013, 303, 95-99.	1.4	38
70	Correlation of microstructural, textural characteristics and hardness of Ti–6Al–4V sheet β-cooled at different rates. Journal of Materials Science, 2020, 55, 8346-8362.	3.7	38
71	A finite-element analysis of the inelastic relaxation of thermal residual stress in continuous-fiber-reinforced composites. Composites Science and Technology, 2001, 61, 1757-1772.	7.8	37
72	Combination of back stress strengthening and Orowan strengthening in bimodal structured Fe–9Cr–Al ODS steel with high Al addition. Materials Science & Engineering A: Structural Materials: Properties, Microstructure and Processing, 2019, 739, 45-52.	5.6	37

#	Article	IF	CITATIONS
73	Neutron diffraction study of stress-induced martensitic transformation and variant change in Fe–Pd. Acta Materialia, 2003, 51, 6453-6464.	7.9	36
74	Elastic strains in antler trabecular bone determined by synchrotron X-ray diffraction. Acta Biomaterialia, 2008, 4, 1677-1687.	8.3	36
75	Lattice strain evolution in IMI 834 under applied stress. Materials Science & Engineering A: Structural Materials: Properties, Microstructure and Processing, 2003, 340, 272-280.	5.6	35
76	Residual stresses in a quenched superalloy turbine disc: Measurements and modeling. Metallurgical and Materials Transactions A: Physical Metallurgy and Materials Science, 2006, 37, 459-467.	2.2	35
77	Study of internal strain evolution in Zircaloy-2 using polycrystalline models: Comparison between a rate-dependent and a rate-independent formulation. Acta Materialia, 2010, 58, 3313-3325.	7.9	35
78	Application of quenching to create highly triaxial residual stresses in type 316H stainless steels. International Journal of Mechanical Sciences, 2006, 48, 235-243.	6.7	34
79	Stress-induced martensitic transformation in Cu–Al–Zn–Mn polycrystal investigated by two in-situ neutron diffraction techniques. Materials Science & Engineering A: Structural Materials: Properties, Microstructure and Processing, 2002, 324, 225-234.	5.6	33
80	Irradiation damage and hardening in pure Zr and Zr-Nb alloys at 573†K from self-ion irradiation. Materials and Design, 2019, 161, 147-159.	7.0	33
81	Interphase and intergranular stress generation in composites exhibiting plasticity in both phases. Acta Materialia, 2005, 53, 2805-2813.	7.9	32
82	Internal Stresses in Deformed Crystalline Aggregates. Reviews in Mineralogy and Geochemistry, 2006, 63, 427-458.	4.8	32
83	Fracture of a minority phase at a stress concentration observed with synchrotron X-ray diffraction. Scripta Materialia, 2009, 61, 939-942.	5.2	32
84	Phase transformation temperatures of Zr alloy Excel. Journal of Nuclear Materials, 2013, 435, 241-249.	2.7	32
85	Orientation-dependent irradiation hardening in pure Zr studied by nanoindentation, electron microscopies, and crystal plasticity finite element modeling. International Journal of Plasticity, 2020, 124, 133-154.	8.8	32
86	Observation of growth of a precipitate at a stress concentration by synchrotron X-ray diffraction. Scripta Materialia, 2010, 62, 341-344.	5.2	31
87	Prediction and measurement of residual stresses in quenched stainless-steel spheres. Materials Science & Engineering A: Structural Materials: Properties, Microstructure and Processing, 2004, 373, 339-349.	5.6	30
88	Stress induced martensite transformation in Co–28Cr–6Mo alloy during room temperature deformation. Materials Science & Engineering A: Structural Materials: Properties, Microstructure and Processing, 2013, 580, 209-216.	5.6	30
89	Atomistic simulations of the formation of <c>-component dislocation loops in α-zirconium. Journal of Nuclear Materials, 2016, 478, 125-134.</c>	2.7	30
90	A new stroboscopic neutron diffraction method for monitoring materials subjected to cyclic loads: Thermal cycling of metal matrix composites. Scripta Materialia, 1996, 35, 717-720.	5.2	29

#	Article	IF	CITATIONS
91	Temperature Dependence of the Activity of Deformation Modes in an HCP Zirconium Alloy. Metallurgical and Materials Transactions A: Physical Metallurgy and Materials Science, 2013, 44, 4183-4193.	2.2	29
92	Irradiation induced microstructural changes in Zr-Excel alloy. Journal of Nuclear Materials, 2013, 441, 138-151.	2.7	29
93	Micromechanical modelling of twinning in polycrystalline materials: Application to magnesium. International Journal of Plasticity, 2016, 85, 156-171.	8.8	29
94	Determination of very low concentrations of hydrogen in zirconium alloys by neutron imaging. Journal of Nuclear Materials, 2018, 503, 98-109.	2.7	29
95	Measurement and modelling of residual stresses in straightened commercial eutectoid steel rods. Acta Materialia, 2005, 53, 4415-4425.	7.9	27
96	The correlation between plastic strain and anisotropy strain in aluminium alloy polycrystals. Materials Science & Engineering A: Structural Materials: Properties, Microstructure and Processing, 2002, 334, 41-48.	5.6	26
97	Dislocation-accelerated void formation under irradiation in zirconium. Acta Materialia, 2015, 82, 94-99.	7.9	26
98	Accumulation of dislocation loops in the $\hat{l}\pm$ phase of Zr Excel alloy under heavy ion irradiation. Journal of Nuclear Materials, 2017, 491, 232-241.	2.7	25
99	Analysis of neutron diffraction strain measurement data from a round robin sample. Journal of Strain Analysis for Engineering Design, 2002, 37, 73-85.	1.8	24
100	Load transfer in bovine plexiform bone determined by synchrotron x-ray diffraction. Journal of Materials Research, 2008, 23, 543-550.	2.6	24
101	Elevated temperature irradiation damage in CANDU spacer material Inconel X-750. Journal of Nuclear Materials, 2014, 445, 227-234.	2.7	24
102	Elastic and plastic properties of \hat{l}^2 Zr at room temperature. Journal of Nuclear Materials, 2009, 393, 67-76.	2.7	23
103	Twinning in structural material with a hexagonal close-packed crystal structure. Journal of Strain Analysis for Engineering Design, 2010, 45, 377-390.	1.8	23
104	The effect of γ′ size and alloy chemistry on dynamic strain ageing in advanced polycrystalline nickel base superalloys. Materials Science & Engineering A: Structural Materials: Properties, Microstructure and Processing, 2013, 573, 54-61.	5.6	23
105	Orientation dependent evolution of plasticity of irradiated Zr-2.5Nb pressure tube alloy studied by nanoindentation and finite element modeling. Journal of Nuclear Materials, 2018, 512, 371-384.	2.7	23
106	Atomistic simulations of Ni segregation to irradiation induced dislocation loops in Zr-Ni alloys. Acta Materialia, 2017, 140, 56-66.	7.9	22
107	A test of a phenomenological model of size dependent melting in Au nanoparticles. Acta Materialia, 2017, 136, 11-20.	7.9	22
108	Dislocation evolution at a crack-tip in a hexagonal close packed metal under plane-stress conditions. Acta Materialia, 2019, 164, 25-38.	7.9	22

#	Article	IF	CITATIONS
109	Thermal residual stresses in NiAl–AlN–Al2O3 composites measured by neutron diffraction. Materials Science & Engineering A: Structural Materials: Properties, Microstructure and Processing, 1999, 264, 108-121.	5.6	21
110	Neutron Diffraction Study of Extruded Magnesium during Cyclic and Elevated Temperature Loading. Materials Science Forum, 2005, 490-491, 257-262.	0.3	21
111	The role of chemical free energy and elastic strain in the nucleation of zirconium hydride. Journal of Nuclear Materials, 2013, 441, 395-401.	2.7	21
112	Stability of Ni3(Al, Ti) Gamma Prime Precipitates in a Nickel-Based Superalloy Inconel X-750 Under Heavy Ion Irradiation. Metallurgical and Materials Transactions A: Physical Metallurgy and Materials Science, 2014, 45, 3422-3428.	2.2	21
113	Contribution on the phase equilibria in Zr–Nb–Fe system. Journal of Nuclear Materials, 2015, 466, 627-633.	2.7	21
114	Quantifying the effect of hydride microstructure on zirconium alloys embrittlement using image analysis. Journal of Nuclear Materials, 2021, 547, 152817.	2.7	21
115	The determination of a stress-free lattice parameter within a stressed material using elastic anisotropy. Journal of Applied Crystallography, 2001, 34, 263-270.	4.5	20
116	Evolution of lattice strain and phase transformation of \hat{I}^2 III Ti alloy during room temperature cyclic tension. Acta Materialia, 2013, 61, 6830-6842.	7.9	20
117	Study of microstructure and precipitates of a Zr-2.5Nb-0.5Cu CANDUÂspacer material. Journal of Nuclear Materials, 2016, 481, 153-163.	2.7	20
118	Hydride Platelet Reorientation in Zircaloy Studied with Synchrotron Radiation Diffraction. Journal of ASTM International, 2011, 8, 1-17.	0.2	20
119	On the determination of single-crystal plasticity parameters by diffraction: optimization of a polycrystalline plasticity model using a genetic algorithm. Journal of Applied Crystallography, 2012, 45, 627-643.	4.5	19
120	Effects of alloying elements on the formation of < <i>c</i> >-component loops in Zr alloy Excel under heavy ion irradiation. Journal of Materials Research, 2015, 30, 1310-1334.	2.6	19
121	Zirconium hydrides and Fe redistribution in Zr-2.5%Nb alloy under ion irradiation. Journal of Nuclear Materials, 2016, 480, 332-343.	2.7	19
122	Effect of pre-existing dislocations on the formation of dislocation loops: Pure magnesium under electron irradiation. Journal of Nuclear Materials, 2018, 511, 43-55.	2.7	19
123	A mechanism for basal vacancy loop formation in zirconium. Scripta Materialia, 2019, 172, 72-76.	5.2	19
124	High-tech composites to ancient metals. Materials Today, 2009, 12, 78-84.	14.2	18
125	Variant selection and transformation texture in zirconium alloy Excel. Journal of Nuclear Materials, 2014, 453, 120-123.	2.7	18
126	Graphene Oxide Membranes for Isotopic Water Mixture Filtration: Preparation, Physicochemical Characterization, and Performance Assessment. ACS Applied Materials & Interfaces, 2020, 12, 34736-34745.	8.0	18

#	Article	IF	CITATIONS
127	Parametric study of stress state development during twinning using 3D finite element modeling. Materials Science & Engineering A: Structural Materials: Properties, Microstructure and Processing, 2011, 528, 2725-2735.	5.6	17
128	Load partitioning and evidence of deformation twinning in dual-phase fine-grained Zr–2.5%Nb alloy. Materials Science & Engineering A: Structural Materials: Properties, Microstructure and Processing, 2013, 564, 548-558.	5.6	17
129	A tomographic TEM study of tension-compression asymmetry response of pyramidal dislocations in a deformed Zr-2.5Nb alloy. Scripta Materialia, 2018, 153, 94-98.	5.2	17
130	Using neutron diffraction measurements to characterize the mechanical properties of polymineralic rocks. Mineralogical Magazine, 2003, 67, 967-987.	1.4	16
131	Intergranular Stress Evolution in Titanium Studied by Neutron Diffraction and Self-consistent Modelling. Journal of Neutron Research, 2004, 12, 33-37.	1.1	16
132	Mapping of crack tip strains and twinned zone in a hexagonal close packed zirconium alloy. Acta Materialia, 2010, 58, 1578-1588.	7.9	16
133	Influence of prior dislocation structure on anisotropy of thermal creep of cold-worked Zr–2.5Nb tubes. Journal of Nuclear Materials, 2011, 412, 138-144.	2.7	16
134	Effect of foil orientation on damage accumulation during irradiation in magnesium and annealing response of dislocation loops. Journal of Nuclear Materials, 2012, 423, 132-141.	2.7	16
135	Radiation induced microstructures in ODS 316 austenitic steel under dual-beam ions. Journal of Nuclear Materials, 2014, 455, 242-247.	2.7	16
136	Evolution of dislocation density in a hot rolled Zr–2.5Nb alloy with plastic deformation studied by neutron diffraction and transmission electron microscopy. Philosophical Magazine, 2017, 97, 2888-2914.	1.6	16
137	Effect of cyclic plasticity on internal stresses in a metal matrix composite. Metallurgical and Materials Transactions A: Physical Metallurgy and Materials Science, 2006, 37, 1977-1986.	2.2	15
138	A furnace with rotating load frame for in situ high temperature deformation and creep experiments in a neutron diffraction beam line. Review of Scientific Instruments, 2012, 83, 053901.	1.3	15
139	Contrast factors of irradiation-induced dislocation loops in hexagonal materials. Journal of Applied Crystallography, 2016, 49, 2184-2200.	4.5	15
140	The habit plane of ã€`a〉-type dislocation loops in α-zirconium: an atomistic study. Philosophical Magazine, 2017, 97, 944-956.	1.6	15
141	In situ monitoring of thermally cycled metal matrix composites by neutron diffraction and laser extensometry. Applied Composite Materials, 1997, 4, 375-392.	2.5	14
142	A new belt-type apparatus for neutron-based rheological measurements at gigapascal pressures. High Pressure Research, 2005, 25, 107-118.	1.2	14
143	A new apparatus for measuring mechanical properties at moderate confining pressures in a neutron beamline. Journal of Applied Crystallography, 2006, 39, 222-229.	4.5	14
144	Influence of short time anneal on recoverable strain of beta III titanium alloy. Materials Science & Engineering A: Structural Materials: Properties, Microstructure and Processing, 2013, 562, 172-179.	5.6	14

#	Article	IF	CITATIONS
145	Nano-scale Mechanical Properties and Microstructure of Irradiated X-750 Ni-Based Superalloy. Metallurgical and Materials Transactions A: Physical Metallurgy and Materials Science, 2018, 49, 498-514.	2.2	14
146	Characterizing the crystal structure and formation induced plasticity of Î ³ -hydride phase in zirconium. Materialia, 2019, 8, 100454.	2.7	14
147	Cavity morphology in a Ni based superalloy under heavy ion irradiation with cold pre-injected helium. I. Journal of Applied Physics, 2014, 115, 103508.	2.5	13
148	Deformation mechanism study of a hot rolled Zr-2.5Nb alloy by transmission electron microscopy. I. Dislocation microstructures in as-received state and at different plastic strains. Journal of Applied Physics, 2015, 117, 094307.	2.5	13
149	Microstructural evaluation and crystallographic texture modification of heat-treated zirconium Excel pressure tube material. Journal of Alloys and Compounds, 2016, 687, 1021-1033.	5.5	13
150	Metastable phases in Zr-Excel alloy and their stability under heavy ion (Kr2+) irradiation. Journal of Nuclear Materials, 2016, 469, 9-19.	2.7	13
151	Stacking faults observed in {10 <mml:math <br="" xmlns:mml="http://www.w3.org/1998/Math/MathML">altimg="si1.gif" overflow="scroll"><mml:mover accent="true"><mml:mn>1</mml:mn><mml:mo stretchy="true">â^²</mml:mo </mml:mover></mml:math> 2} extension twins in a compressed high Sn content Zr allov. Scripta Materialia. 2017. 141. 72-75.	5.2	13
152	Precipitate Stability in a Zr–2.5Nb–0.5Cu Alloy under Heavy Ion Irradiation. Metals, 2017, 7, 287.	2.3	13
153	<i>In situ</i> transmission electron microscopy study of the thermally induced formation of δ′-ZrO in pure Zr and Zr-based alloy. Journal of Applied Crystallography, 2017, 50, 1028-1035.	4.5	13
154	Radiation effect on nano-indentation properties and deformation mechanisms of a Ni-based superalloy X-750. Journal of Nuclear Materials, 2019, 515, 1-13.	2.7	13
155	The Effect of Lattice Misfit on Deformation Mechanisms at High Temperature. Advanced Materials Research, 0, 278, 144-149.	0.3	12
156	Lattice strains and load partitioning in bovine trabecular bone. Acta Biomaterialia, 2011, 7, 716-723.	8.3	12
157	Discovery of a ã€^2 1 0〉-fiber texture in medical-grade metastable beta titanium wire. Acta Materialia, 2015, 87, 390-398.	7.9	12
158	Micropillar compression study on heavy ion irradiated Zr-2.5Nb pressure tube alloy. Journal of Nuclear Materials, 2018, 511, 487-495.	2.7	12
159	Investigation of <mml:math <br="" xmlns:mml="http://www.w3.org/1998/Math/MathML">altimg="si2.svg"><mml:mi>Î</mml:mi></mml:math> zirconium hydride morphology in a single crystal using quantitative phase field simulations supported by experiments. Journal of Nuclear Materials, 2021. 557. 153303.	2.7	12
160	Mechanisms of Hydride Reorientation in Zircaloy-4 Studied in Situ. , 2015, , 1107-1137.		12
161	Identifying the true structure and origin of the water-quench induced hydride phase in Zr-2.5Nb alloy. Acta Materialia, 2021, 221, 117369.	7.9	12
162	Examination of tensile/compressive loading asymmetries in aluminium based metal matrix composites using finite element method. Materials Science and Technology, 1995, 11, 228-235.	1.6	11

#	Article	IF	CITATIONS
163	The blurring in strains measured at a pulsed neutron source introduced by the use of a detector with a large angular coverage. Physica B: Condensed Matter, 2001, 301, 221-226.	2.7	11
164	Neutron diffraction study of the deformation behaviour of deformation processed copper–chromium composites. Materials Science & Engineering A: Structural Materials: Properties, Microstructure and Processing, 2003, 348, 208-216.	5.6	11
165	Comparison of experimentally determined texture development in Zircaloy-2 with predictions from a rate-dependent polycrystalline model. Materials Science & Engineering A: Structural Materials: Properties, Microstructure and Processing, 2011, 528, 8676-8686.	5.6	11
166	Measurement and modeling of strain fields in zirconium hydrides precipitated at a stress concentration. Journal of Nuclear Materials, 2012, 430, 27-36.	2.7	11
167	Cavity morphology in a Ni based superalloy under heavy ion irradiation with hot pre-injected helium. II. Journal of Applied Physics, 2014, 115, 103509.	2.5	11
168	Evidence for deformation-induced phase transformation in a high Sn content zirconium alloy. Acta Materialia, 2018, 161, 311-319.	7.9	11
169	A direct comparison of annealing in TEM thin foils and bulk material: Application to Zr-2.5Nb-0.5Cu alloy. Materials Characterization, 2019, 151, 175-181.	4.4	11
170	Influence of Al Addition Strategy on the Microstructure of a Lowâ€Cr Oxide Dispersionâ€Strengthened Ferritic Steel. Advanced Engineering Materials, 2020, 22, 1900879.	3.5	11
171	Stability of vacancy and interstitial dislocation loops in <mml:math xmlns:mml="http://www.w3.org/1998/Math/MathML" altimg="si24.svg"><mml:mi>α</mml:mi>-zirconium: atomistic calculations and continuum modelling. lournal of Nuclear Materials. 2021. 554. 153059.</mml:math 	2.7	11
172	Primary damage production in the presence of extended defects and growth of vacancy-type dislocation loops in hcp zirconium. Physical Review Materials, 2019, 3, .	2.4	11
173	An experimental test of a neutron silicon lens. Nuclear Instruments and Methods in Physics Research, Section A: Accelerators, Spectrometers, Detectors and Associated Equipment, 2002, 485, 606-614.	1.6	10
174	Strain-induced phase transformation in a cobalt-based superalloy during different loading modes. Materials Science & Engineering A: Structural Materials: Properties, Microstructure and Processing, 2011, 528, 6051-6058.	5.6	10
175	Orientation relationships between α-zirconium and δ-hydride within a hydride blister. Journal of Applied Crystallography, 2017, 50, 349-356.	4.5	10
176	Synchrotron X-ray diffraction study of zirconium hydride distribution in Zr-2.5%Nb and its redistribution during thermal cycling. Materials Characterization, 2018, 136, 183-195.	4.4	10
177	Crack propagation path selection and plastic deformation at a crack tip in zirconium. Materials Science & Engineering A: Structural Materials: Properties, Microstructure and Processing, 2020, 779, 139143.	5.6	10
178	Towards resolving a long existing phase stability controversy in the Zr-H, Ti-H systems. Journal of Nuclear Materials, 2021, 543, 152540.	2.7	10
179	Deep learning and crystal plasticity: A preconditioning approach for accurate orientation evolution prediction. Computer Methods in Applied Mechanics and Engineering, 2022, 389, 114392.	6.6	10
180	Neutron-diffraction study of martensitic transformation in austenitic stainless steel under low-cycling tensile-compressive loading. Applied Physics A: Materials Science and Processing, 2002, 74, s1391-s1393.	2.3	9

#	Article	IF	CITATIONS
181	Orientation dependence of martensite variants during loading of Fe–Pd shape memory alloy. Scripta Materialia, 2005, 53, 609-612.	5.2	9
182	Comparison using neutron diffraction of martensitic transformation in Fe–Mn–Si shape memory alloys with and without VN precipitates. Materials Science and Technology, 2008, 24, 902-907.	1.6	9
183	Evolution of internal strains in a two phase zirconium alloy during cyclic loading. Acta Materialia, 2011, 59, 5305-5319.	7.9	9
184	A modified Rietveld method to model highly anisotropic ceramics. Acta Materialia, 2012, 60, 1494-1502.	7.9	9
185	The Zr20Nb–H phase diagram and the characterisation of hydrides in β-Zr. Journal of Nuclear Materials, 2013, 442, 292-297.	2.7	9
186	Deformation mechanism study of a hot rolled Zr-2.5Nb alloy by transmission electron microscopy. II. <i>In situ</i> transmission electron microscopy study of deformation mechanism change of a Zr-2.5Nb alloy upon heavy ion irradiation. Journal of Applied Physics, 2015, 117, .	2.5	9
187	Crystallographic texture and microstructural changes in fusion welds of recrystallized Zry-4 rolled plates. Journal of Nuclear Materials, 2017, 488, 83-99.	2.7	9
188	Re-investigation of phase transformations in the Zr-Excel alloy. Journal of Alloys and Compounds, 2017, 716, 7-12.	5.5	9
189	Retention of metastable β phase in a two-phase quaternary zirconiumÂalloy. Materials and Design, 2018, 156, 622-630.	7.0	9
190	Effect of the addition of Cu on irradiation induced defects and hardening in Zr-Nb alloys. Journal of Nuclear Materials, 2019, 519, 10-21.	2.7	9
191	Crystallographic orientation sensitive measurement of strain rate sensitivity in Zircaloy-2 via synchrotron X-ray diffraction. International Journal of Plasticity, 2019, 113, 1-17.	8.8	9
192	Effect of He on the Order-Disorder Transition in Ni3Al under Irradiation. Physical Review Letters, 2020, 124, 075901.	7.8	9
193	Atomistic structure and thermal stability of dislocation loops, stacking fault tetrahedra, and voids in face-centered cubic Fe. Journal of Nuclear Materials, 2022, 563, 153636.	2.7	9
194	Interplay of stresses induced by phase transformation and plastic deformation during cyclic load of austenitic stainless steel. Physica B: Condensed Matter, 2004, 350, 98-101.	2.7	8
195	Effects of Texture and Anisotropy on Intergranular Stress Development in Zirconium. Materials Science Forum, 2005, 495-497, 1553-1558.	0.3	8
196	Deformation-induced phase development in a cobalt-based superalloy during monotonic and cyclic deformation. Physica B: Condensed Matter, 2006, 385-386, 523-525.	2.7	8
197	Effect of heat treatment temperature on nitinol wire. Applied Physics Letters, 2014, 105, .	3.3	8
198	Formation mechanisms of periodic longitudinal microstructure and texture patterns in friction stir welded magnesium AZ80. Materials Characterization, 2016, 122, 22-29.	4.4	8

#	Article	IF	CITATIONS
199	Strain localisation and failure of dissimilar magnesium-based alloy friction stir welds. Science and Technology of Welding and Joining, 2018, 23, 628-634.	3.1	8
200	Asymmetrical response of edge pyramidal dislocations in HCP zirconium under tension and compression: A molecular dynamics study. Computational Materials Science, 2019, 170, 109183.	3.0	8
201	Comparison of electron backscatter and X-ray diffraction techniques for measuring dislocation density in Zircaloy-2. Journal of Applied Crystallography, 2019, 52, 415-427.	4.5	8
202	The dependence of damage accumulation on irradiation dose rate in zirconium alloys: Rate theory, atomistic simulation and experimental validation. Journal of Nuclear Materials, 2021, 543, 152478.	2.7	8
203	Seeing through Corrosion: Using Micro-focus X-ray Computed Tomography and Neutron Computed Tomography to Digitally "Clean―Ancient Bronze Coins. Materials Research Society Symposia Proceedings, 2011, 1319, 1.	0.1	7
204	Irradiation damage in commercial purity magnesium. Nuclear Instruments & Methods in Physics Research B, 2012, 272, 231-235.	1.4	7
205	Aging response and characterization of precipitates in Zr alloy Excel pressure tube material. Journal of Nuclear Materials, 2014, 452, 265-272.	2.7	7
206	Evolution of Intergranular Stresses in a Martensitic and an Austenitic NiTi Wire During Loading–Unloading Tensile Deformation. Metallurgical and Materials Transactions A: Physical Metallurgy and Materials Science, 2015, 46, 2476-2490.	2.2	7
207	Crystal plasticity modeling of damage accumulation in dissimilar Mg alloy bi-crystals under high-cycle fatigue. International Journal of Fatigue, 2016, 90, 99-108.	5.7	7
208	Influence of magnesium AZ80 friction stir weld texture on tensile strain localisation. Materials Science and Technology, 2017, 33, 189-199.	1.6	7
209	Thermal creep behavior in heat-treated and modified textured Zr-Excel pressure tube material. Materials Science & Engineering A: Structural Materials: Properties, Microstructure and Processing, 2017, 698, 326-340.	5.6	7
210	The stability of thermodynamically metastable phases in a Zr-Sn-Nb-Mo alloy: Effects of alloying elements, morphology and applied stress/strain. Journal of Nuclear Materials, 2017, 493, 84-95.	2.7	7
211	Study on the morphology of bulk hydrides by synchrotron X-ray tomography. Materials Characterization, 2017, 134, 362-369.	4.4	7
212	Strain evolution in Zr-2.5†wt% Nb observed with synchrotron X-ray diffraction. Materials Characterization, 2018, 146, 35-46.	4.4	7
213	The neutron silicon lens: a new lens design for thermal neutrons. Physica B: Condensed Matter, 2000, 283, 308-313.	2.7	6
214	Time-of-flight neutron-diffraction investigations of elastic and anisotropy strains in fatigued austenitic stainless steel. Applied Physics A: Materials Science and Processing, 2002, 74, s1385-s1387.	2.3	6
215	Micromechanics of stress-induced martensitic transformation. Materials Science & Engineering A: Structural Materials: Properties, Microstructure and Processing, 2004, 378, 479-483.	5.6	6
216	Evolution of Interphase Stress in Zr-2.5%Nb during Deformation. Advanced Materials Research, 2006, 15-17, 615-620.	0.3	6

#	Article	IF	CITATIONS
217	Evolution of lattice strains in three dimensions during in situ compression of textured Zircaloy-2. Journal of Neutron Research, 2007, 15, 121-130.	1.1	6
218	Quasi in-situ energy dispersive X-ray spectroscopy observation of matrix and solute interactions on Y Ti O oxide particles in an austenitic stainless steel under 1ÂMeV Kr2+ high temperature irradiation. Acta Materialia, 2017, 141, 241-250.	7.9	6
219	Modeling of particle coarsening and precipitation free zones. Modelling and Simulation in Materials Science and Engineering, 2017, 25, 085012.	2.0	6
220	Irradiation Induced Defect Clustering in Zircaloy-2. Applied Sciences (Switzerland), 2017, 7, 854.	2.5	6
221	<i>In situ</i> heavy ion irradiation in ferritic/martensitic ODS steels at 500°C. Materials Science and Technology, 2018, 34, 42-46.	1.6	6
222	Mode I fracture testing validation on non-plane strain zirconium foils. Engineering Fracture Mechanics, 2019, 209, 48-60.	4.3	6
223	In-situ study of heavy ion irradiation induced lattice defects and phase instability in β-Zr of a Zr–Nb alloy. Journal of Nuclear Materials, 2019, 522, 192-199.	2.7	6
224	In situ TEM and multiscale study of dislocation loop formation in the vicinity of a grain boundary. Journal of Nuclear Materials, 2020, 528, 151872.	2.7	6
225	Transformation behavior of hydrides precipitated with or without stress in Zr-2.5Nb investigated by in-situ S/TEM thermal cycling. Journal of Nuclear Materials, 2021, 559, 153428.	2.7	6
226	Diffusion of H in Zircaloy-2 and Zr-2.5%Nb rolled plates between 250°C and 350°C by off-situ neutron imaging experiments. Journal of Nuclear Materials, 2022, 561, 153547.	2.7	6
227	New insights into the structure and chemical reduction of graphene oxide membranes for use in isotopic water separations. Journal of Membrane Science, 2022, 659, 120785.	8.2	6
228	Stress induced martensitic transformation in CuAlZnMn polycrystals investigated by in situ neutron diffraction. European Physical Journal Special Topics, 2001, 11, Pr8-159-Pr8-166.	0.2	5
229	Effect of Cyclic Loading on Strain Distribution in a Particulate-Reinforced Metal Matrix Composite. Materials Science Forum, 2002, 404-407, 541-546.	0.3	5
230	Mechanical energy criterion for stress-induced martensitic transformation. Scripta Materialia, 2003, 49, 1013-1019.	5.2	5
231	Silicon APS detectors for neutron scattering. Nuclear Instruments and Methods in Physics Research, Section A: Accelerators, Spectrometers, Detectors and Associated Equipment, 2003, 501, 72-79.	1.6	5
232	Neutron diffraction study of stress-induced martensitic transformation and variant change in Fe–Pd shape memory alloy. Materials Science & Engineering A: Structural Materials: Properties, Microstructure and Processing, 2004, 378, 328-332.	5.6	5
233	Fatigue-induced phase formation and its deformation behavior in a cobalt-based superalloy. Powder Diffraction, 2005, 20, 121-124.	0.2	5
234	Methodology and recent developments for using neutron diffraction to characterize the mechanical properties of rocks. Physica B: Condensed Matter, 2006, 385-386, 938-941.	2.7	5

#	Article	IF	CITATIONS
235	Effect of loading mode on lattice strain measurements via neutron diffraction. Materials Science & Engineering A: Structural Materials: Properties, Microstructure and Processing, 2013, 577, 169-178.	5.6	5
236	Monitoring in situ stress/strain behaviour during plastic yielding in polymineralic rocks using neutron diffraction. Journal of Structural Geology, 2013, 47, 36-51.	2.3	5
237	Microstructure evolution during electron and ion irradiation in commercial purity magnesium. Philosophical Magazine, 2014, 94, 1909-1923.	1.6	5
238	Effect of heavy ion irradiation on thermodynamically equilibrium Zr-Excel alloy. Journal of Nuclear Materials, 2017, 488, 33-45.	2.7	5
239	An embedded atom method interatomic potential for the zirconium-iron system. Computational Materials Science, 2017, 133, 6-13.	3.0	5
240	Advanced Characterization of Hydrides in Zirconium Alloys. Minerals, Metals and Materials Series, 2019, , 1793-1813.	0.4	5
241	Evaluation of irradiation hardening in proton-irradiated <mml:math xmlns:mml="http://www.w3.org/1998/Math/MathML" altimg="si1.svg"><mml:mi>δ</mml:mi>-zirconium hydride and Zr2.5Nb. Journal of Nuclear Materials. 2022. 562. 153600.</mml:math 	2.7	5
242	The Development of Strain Anisotropy during Plastic Deformation of an Aluminium Polycrystal. Materials Science Forum, 2000, 347-349, 492-497.	0.3	4
243	Residual Stress Analysis of Fatigued Austenitic Stainless Steel. Journal of Neutron Research, 2003, 11, 255-261.	1.1	4
244	Effect of interstitial oxygen and iron on deformation of Zr–2.5 wt% Nb. Materials Science & Engineering A: Structural Materials: Properties, Microstructure and Processing, 2015, 636, 10-23.	5.6	4
245	Phase Transformation Temperatures and Solute Redistribution in a Quaternary Zirconium Alloy. Metallurgical and Materials Transactions A: Physical Metallurgy and Materials Science, 2018, 49, 3468-3485.	2.2	4
246	A synchrotron X-ray diffraction study of strain and microstrain distributions in α-Zr caused by hydride precipitation. Surfaces and Interfaces, 2019, 17, 100388.	3.0	4
247	Effect of rate on the deformation properties of metastable β in a high Sn content zirconium alloy. International Journal of Plasticity, 2019, 119, 102-122.	8.8	4
248	Investigation on the deformation mechanisms and size-dependent hardening effect of He bubbles in 84â€ ⁻ dpa neutron irradiated Inconel X-750. Nuclear Materials and Energy, 2021, 28, 101025.	1.3	4
249	Title is missing!. Applied Composite Materials, 1997, 4, 375-393.	2.5	3
250	The expected uncertainty of diffraction-peak location. Applied Physics A: Materials Science and Processing, 2002, 74, s112-s114.	2.3	3
251	An Analysis of Lattice Strain due to Disclination Dipole Walls in Fe-Pd Martensite. Journal of Neutron Research, 2004, 12, 39-44.	1.1	3
252	Investigation of mechanical features of low cycle fatigue specimens of austenitic steel AISI type 321 under applied load by neutron diffraction stress analysis. Materials Science and Technology, 2005, 21, 35-45.	1.6	3

#	Article	IF	CITATIONS
253	Using neutrons to investigate changes in strain partitioning between the phases during plastic yielding of calcite+halite composites. Physica B: Condensed Matter, 2006, 385-386, 946-948.	2.7	3
254	The Effect of Plastic Anisotropy on the Residual Stress within a 316L Stainless Steel Bead-on-Plate Specimen. Materials Science Forum, 2006, 524-525, 679-684.	0.3	3
255	Neutron Strain Scanning of Archaeological Bronzes. Materials Science Forum, 2006, 524-525, 975-980.	0.3	3
256	Novel techniques of preparing TEM samples for characterization of irradiation damage. Journal of Microscopy, 2013, 252, 251-257.	1.8	3
257	On the predictions of self-consistent plasticity models: The effect of loading mode during in situ diffraction tests. Materials Science & Engineering A: Structural Materials: Properties, Microstructure and Processing, 2015, 634, 77-85.	5.6	3
258	Quantitative characterization of the microstructure of heat-treated Zr-Excel by neutron line profile analysis. Journal of Applied Crystallography, 2016, 49, 1609-1623.	4.5	3
259	Effect of temperature and loading sense on deformation-induced phase transformation in a high Sn content zirconium alloy. Materials Science & Engineering A: Structural Materials: Properties, Microstructure and Processing, 2019, 748, 313-326.	5.6	3
260	A method for calculation of bias factor in anisotropic mediums, application to αâ^'zirconium. Journal of Nuclear Materials, 2020, 528, 151882.	2.7	3
261	Phase Transformation and Atypical Variants in an Extruded Two Phase Zirconium Tube. Metallurgical and Materials Transactions A: Physical Metallurgy and Materials Science, 2020, 51, 2724-2737.	2.2	3
262	In Situ Studies of Variant Selection During the α-β-α Phase Transformation in Zr-2.5Nb. Journal of ASTM International, 2011, 8, 1-14.	0.2	3
263	High temperature hardness testing of <mml:math <br="" xmlns:mml="http://www.w3.org/1998/Math/MathML">altimg="si4.svg"><mml:mi>î´</mml:mi></mml:math> -zirconium hydride: Yield stress estimation by analytical and numerical models. Journal of Nuclear Materials, 2022, 560, 153424.	2.7	3
264	Characterization of microstructure and microhardness of Neutron irradiated Inconel X-750. Journal of Nuclear Materials, 2022, 563, 153644.	2.7	3
265	Radiation-induced segregation on dislocation loops in austenitic Fe-Cr-Ni alloys. Physical Review Materials, 2022, 6, .	2.4	3
266	Measurement of the residual stresses near a short 20° repair in a 19 mm thick stainless steel pipe girth weld. Journal of Neutron Research, 2001, 9, 173-180.	1.1	2
267	The sin2 Ï^-method in pulsed neutron transmission. Journal of Neutron Research, 2001, 9, 289-294.	1.1	2
268	Neutron Diffraction Study of Plasticity-Induced Martensite Formation of the Austenitic Stainless Steel AISI 321. Materials Science Forum, 2002, 404-407, 501-508.	0.3	2
269	Neutron strain scanning in straightened eutectoid steel rods. Applied Physics A: Materials Science and Processing, 2002, 74, s1679-s1682.	2.3	2
270	Intergranular strains in transforming NiTi alloys. IEEE Transactions on Nuclear Science, 2005, 52, 326-329.	2.0	2

#	Article	IF	CITATIONS
271	16. Internal Stresses in Deformed Crystalline Aggregates. , 2006, , 427-458.		2
272	Effects of heavy ion irradiation on Zr-2.5Nb pressure tube alloy. I. Orientation dependent mechanical response. Journal of Applied Physics, 2019, 125, .	2.5	2
273	Phase transformation and microstructural changes during the hydriding and aging processes in dual phase Zr alloy. Materials Chemistry and Physics, 2019, 231, 48-59.	4.0	2
274	Effects of heavy ion irradiation on Zr-2.5Nb pressure tube alloy. II. Orientation dependent dislocation loop propagation and elemental redistribution. Journal of Applied Physics, 2019, 125, .	2.5	2
275	High-Resolution Residual Stress Mapping of Magnesium AZ80 Friction Stir Welds for Three Processing Conditions. Metallurgical and Materials Transactions A: Physical Metallurgy and Materials Science, 2020, 51, 1195-1207.	2.2	2
276	Effects of Heat Treatment on CANDU® Pressure Tube Electrical Resistivity. Journal of Nuclear Materials, 2021, 545, 152597.	2.7	2
277	Crystal Structure of Hydride Platelets in Hot Rolled Zircaloy-2, Characterized with Synchrotron X-Ray Diffraction, S/TEM, and EELS. , 2021, , 732-761.		2
278	Advanced Characterization of Hydrides in Zirconium Alloys. Minerals, Metals and Materials Series, 2018, , 577-597.	0.4	2
279	Characterization of Zr-Nb-Fe(-Cr) precipitates in Zr-based alloys using density functional theory. Materials Today Communications, 2022, 31, 103381.	1.9	2
280	The determination of d0 without a reference material. Journal of Neutron Research, 2001, 9, 469-479.	1.1	1
281	Mechanical characterisation of fatigued austenitic stainless steel under applied loads by in-situ neutron diffraction. Journal of Neutron Research, 2001, 9, 207-215.	1.1	1
282	Creating Highly Triaxial Residual Stresses and Relaxation of the Stress Field due to Thermal Ageing. Journal of Neutron Research, 2004, 12, 111-115.	1.1	1
283	Intergranular Stress Development in Al during Dynamic Strain Ageing. Journal of Neutron Research, 2004, 12, 213-217.	1.1	1
284	Measurement of Residual Stress in a Powder Metallurgy Aluminium-SiC Composite. Journal of Neutron Research, 2004, 12, 129-133.	1.1	1
285	Tensile deformation of a Cu mosaic crystal along the [110] direction studied by time of flight neutron transmission. Materials Science & Engineering A: Structural Materials: Properties, Microstructure and Processing, 2006, 437, 151-156.	5.6	1
286	Fatigue Degradation and Martensitic Transformation of Austenitic Stainless Steel AlSi 321: New Results and Prospects. Materials Science Forum, 2006, 524-525, 899-904.	0.3	1
287	Dynamical diffraction peak splitting in time-of-flight neutron diffraction. Applied Physics Letters, 2006, 89, 233515.	3.3	1
288	Development of Intergranular Stresses during <i>In Situ</i> Compression Tests in Zircaloy-4. Materials Science Forum, 0, 571-572, 149-154.	0.3	1

#	Article	IF	CITATIONS
289	Ultra-small-angle X-ray scattering study of second-phase particles in heat-treated Zircaloy-4. Journal of Applied Crystallography, 2015, 48, 52-60.	4.5	1
290	Determinación de bajas concentraciones de hidrógeno en aleaciones de circonio utilizando radiografÃa de neutrones como técnica no destructiva. Revista Materia, 2018, 23, .	0.2	1
291	Intergranular and Interphase Constraints in Zirconium Alloys. Journal of ASTM International, 2008, 5, 1-20.	0.2	1
292	Hydride Platelet Reorientation in Zircaloy Studied with Synchrotron Radiation Diffraction. , 2012, , 496-522.		1
293	Investigating the stability of reoriented hydrides and their reprecipitation using in-situ heating experiments. Journal of Nuclear Materials, 2022, 564, 153670.	2.7	1
294	Residual stress states before irradiation in ESS target structural materials. Applied Physics A: Materials Science and Processing, 2002, 74, s1197-s1199.	2.3	0
295	Elastoplastic Deformation of Two Phase Steels Studied by Neutron Diffraction and Self-consistent Modelling. , 2002, , 495-506.		0
296	Neutron diffraction characterisation of thermomechanical behaviour of Fe-Mn-Si shape memory alloy. Journal of Neutron Research, 2007, 15, 179-184.	1.1	0
297	Measurement of Hydride Precipitation and Dissolution Kinetics Using Synchrotron X-Rays. , 2016, , .		0
298	Toward a Mechanistic Understanding of Pellet Cladding Interaction Using Advanced 3D Characterization and Atomistic Simulation. , 2021, , 904-926.		0
299	Back-Calculated Indentation Stress-Strain Curves from Small Scale Testing and Verification Using Finite Element Models: Application to Nanoindentation and Micropillar Compression Study of a Heavy Ion Irradiated Zr-2.5Nb Alloy. , 2021, , 294-318.		0
300	Interstitialcy-based reordering kinetics of Ni3Al precipitates in irradiated Ni-based super alloys. Materialia, 2021, 19, 101180.	2.7	0
301	Prediction and Measurement of Residual Stresses Arising From Quenching of Stainless Steels. , 2004, , .		0
302	Measurement of the Strain Distribution in Notch Tip Hydrides With High Energy X-Ray Diffraction and the Impact on Overload Modeling. , 2010, , .		0
303	In Situ Studies of Variant Selection During the α—β—α Phase Transformation in Zr-2.5Nb. , 2012, , 195-215.		0
304	In Situ Studies of Variant Selection During the α—β—α Phase Transformation in Zr-2.5Nb. , 2011, , 195-215.		0
305	In Situ Studies of Variant Selection During the α—β—α Phase Transformation in Zr-2.5Nb. , 2012, , 195-215.		0
306	Hydride Platelet Reorientation in Zircaloy Studied with Synchrotron Radiation Diffraction. , 2011, , 496-522.		0

#	Article	IF	CITATIONS
307	Hydride Platelet Reorientation in Zircaloy Studied with Synchrotron Radiation Diffraction. , 2012, , 496-522.		Ο
308	Hydride Behavior in Zircaloy-4 During Thermomechanical Cycling. , 2011, , 683-688.		0
309	Thermal-Creep Induced Stress Relaxation Near a Notch in Zr-2.5Nb. , 2012, , .		0